

Graph-Theoretic Agreement Framework for Multi-Agent LLM Systems

Muhammad Umar Javed

Amazon Web Services, Seattle, USA
mumarjav@amazon.com

Abstract. The transition from monolithic Large Language Models (LLMs) to distributed, multi-agent architectures necessitates a paradigm shift in how we understand, verify, and secure autonomous coordination. Unlike traditional multi-agent systems, which typically focus on cooperative state alignment and resource sharing, modern LLM patterns—such as multi-agent debate, constitutional oversight, and helper-critic loops—rely heavily on *adversarial critique* as a fundamental mechanism for error correction and reasoning refinement. Furthermore, as LLMs are dynamical systems whose latent mental states are not always perfectly observable from their verbalized outputs, securing these networks requires understanding both macroscopic network topology and microscopic agent observability. This paper establishes a comprehensive, rigorous graph-theoretic framework for analyzing and guaranteeing consensus in these signed, directed interaction networks. We bridge the gap between graph theory and LLM reasoning by formally mapping Transformer cross-entropy log-odds to the signed Laplacian. We characterize the underlying stability of agreement through the lens of structural balance theory, demonstrating how unbalanced critique cycles lead to *logical frustration* and *persistent reasoning oscillations*. We prove that unobservable latent states introduced via *hidden* system prompts act as topological Trojan horses, fundamentally destabilizing cooperative consensus. To resolve these unobservable deadlocks, we restrict the interaction topology to chordal (triangulated) graphs and apply matrix decomposition with Gram-Schmidt orthogonalization. We mathematically prove that rank-one spectral edge perturbations can deterministically break expertise symmetry, strictly shifting eigenvalues into the stable left-half plane. Our core contributions include mathematical consensus theorems, polynomial-time Perfect Elimination Ordering (PEO) verification algorithms, and comprehensive, large-scale empirical validation on clustered ensembles of LLaMA-3, Mistral, and Gemma agents.

A Introduction

The landscape of Generative Artificial Intelligence (GenAI) has undergone a profound transformation over the last three years. The field has evolved from optimizing isolated, monolithic Large Language Models (LLMs) via prompt engineering to the orchestration of complex, distributed societies consisting of multiple, highly specialized AI agents. Frameworks such as *AutoGen* [1], *MetaGPT*

[16], *ChatDev* [15], and *Multi-agent Debate* [2] have empirically demonstrated that the collective output of an interacting ensemble of specialized models frequently surpasses the reasoning capabilities, factuality, and coding proficiency of any single state-of-the-art model acting alone.

However, as we transition these multi-agent systems from experimental, human-in-the-loop pipelines to fully autonomous coordination networks at scale, we encounter a fundamental and largely unsolved problem in computer science: *Under what rigorous, verifiable conditions will a society of language agents reach a stable, unique consensus, especially when the internal mental states of those agents may be unobservable?*

Currently, coordination within LLM societies is implemented through brittle heuristics. Systems engineers rely on arbitrary constraints such as *maximum conversation rounds*, *stop tokens*, or *fixed sequential pipelines* to forcibly terminate interactions that might otherwise never converge. In high-trust autonomous applications—spanning legal reasoning synthesis, automated software architecture generation, medical diagnosis, and scientific discovery—a failure to reach consensus is not merely a matter of computational inefficiency; it constitutes a failure of the system’s reasoning and alignment.

A.1 The Challenge of Adversarial Coordination and Observability

Traditional coordination theory (e.g., through Linda tuple spaces [3], Reo circuits [4], and Actor models) primarily focuses on data flow, event synchronization, and cooperative goal achievement. Similarly, classical multi-agent consensus theory in control systems [5] has predominantly focused on networks of positive influence, where agents seek to minimize the variance between their states to reach a shared physical or logical value.

LLM coordination is fundamentally unique and mathematically complex for two reasons:

1. **Antagonistic Interactions:** LLM societies explicitly and heavily utilize adversarial critique. In a *Multi-agent Debate* [2] or a *Constitutional AI* framework [8], a Critic agent is explicitly incentivized and prompted to identify flaws, oppose assertions, and move the collective reasoning state *away* from the Helper agent’s current position. This is an *honest but adversarial* interaction designed to prune the logical search space.
2. **Partial Observability of Latent States:** Recent work by Liu et al. [9] demonstrates that LLMs are dynamical systems where the internal *mental* state (activations in the embedding space) is not always reconstructible from the verbal state (the output tokens). When models possess hidden system prompts or internal fading memory loops, multiple disparate mental state trajectories can yield the exact same verbal output. Liu et al. analogize these self-contained, unobservable state trajectories to feelings.

The combination of adversarial critique and unobservable mental states requires a radical departure from standard unsigned graph theory. How can a

society of AI agents reach a reliable consensus when some agents are actively pushing the network away from agreement, and the true motives (mental states) of those agents are mathematically hidden?

A.2 Contributions and Paper Structure

This paper addresses this critical gap by fusing *signed graph theory*, *nonlinear observability theory*, and *spectral matrix perturbation* with the latent dynamics of LLM reasoning. We treat the reasoning state of an AI agent as a continuous representation in a high-dimensional latent space and rigorously analyze how reinforcement (positive edge weights) and critique (negative edge weights) dictate the global convergence of the society.

The primary contributions of this paper are:

1. We provide a continuous-time dynamic model for LLM token and reasoning evolution that natively incorporates both cooperative and adversarial influence channels, explicitly mapping Transformer logits to the Laplacian manifold.
2. We introduce the concept of *logical frustration*—adapted from Harary’s social balance theory [6]—proving that unbalanced critique cycles are the mathematical root cause of infinite debate loops and hallucinations in multi-agent networks.
3. We extend the single-agent observability framework of Liu et al. [9] to multi-agent networks, demonstrating how unobservable *feelings* (hidden system prompts) can act as topological Trojan horses, covertly violating structural balance from within a seemingly cooperative cluster.
4. We mathematically prove that overlapping triadic debates (chordal graphs) require strictly asymmetric expertise weights ($w_a \neq w_b$) to converge. Furthermore, we provide a rigorous Gram-Schmidt proof that rank-one spectral edge perturbations guarantee consensus by forcing rogue zero eigenvalues into the stable left-half plane.
5. We present polynomial-time algorithms leveraging Perfect Elimination Orderings (PEO) for autonomous topological pruning, supported by a comprehensive experimental setup evaluating thousands of messaging rounds across LLaMA-3, Mistral, and Gemma agents.

The remainder of this paper is structured as follows. Section 2 provides a comprehensive review of related work. Section 3 formalizes the system model, explicitly connecting Transformer latent logic to the signed LLM Laplacian. Section 4 explores structural balance and logical frustration. Section 5 integrates observability and Trojan dynamics. Section 6 presents the mathematical decomposition of triangulated graphs and the core perturbation proofs. Section 7 generalizes these findings into broader consensus theorems. Section 8 details the algorithmic implementations. Section 9 provides the complete experimental setup and empirical results. Section 10 discusses the limitations of our stochastic assumptions, followed by concluding remarks in Section 11. We provide proofs of all Theorems and results in Appendices.

B Background and Related Work

To fully contextualize the contributions of this framework, we trace the lineage of coordination theory, the mathematics of signed consensus, and the recent breakthroughs in Generative AI observability.

B.1 Traditional Formal Coordination Models

The study of coordination is focused on decoupling computation from communication. Gelernter and Carriero’s Linda [3] introduced generative communication via tuple spaces, abstracting away the identities of interacting agents. Later, Arbab’s Reo [4] provided a compositional paradigm where complex coordination protocols could be built from simple channels. While these models are Turing-complete and capable of orchestrating complex concurrent systems, they inherently treat the data payload as opaque. In LLM societies [13], the *data* consists of highly semantic natural language strings. The coordination logic is inextricably linked to the semantic content; an agent’s internal state update depends entirely on whether it interprets a received message as a corroborating fact or a contradictory critique.

B.2 Signed Graphs and Bipartite Consensus

To model antagonistic interactions, mathematicians rely on signed graphs. Harary [6] introduced the notion of structural balance to model tension in human social networks (e.g., the enemy of my enemy is my friend). Altafini [7] was the first to formalize consensus on dynamically changing antagonistic networks. Altafini proved that if a signed graph is structurally balanced, the agents will reach a *bipartite consensus*—the network divides into two polarized factions where the agents in one faction reach a state x^* , and the agents in the other reach $-x^*$. While bipartite consensus accurately models political polarization, it is generally undesirable in an LLM society deployed to solve a specific mathematical or logical problem [30]. In this paper, we extend Altafini’s work to define the specific constraints required to force a signed, adversarial LLM network to converge to a *unipolar consensus* (total agreement on a single truth).

B.3 Observability, Meanings, and Feelings in LLMs

A critical foundation for our work is the recent formulation of LLMs as dynamical systems by Liu et al. [9]. They define the state space as a sliding window of data and the process of predicting the next token as a state transition.

Crucially, Liu et al. explore whether these models are *observable*—i.e., whether the latent mental state trajectories of the LLM can be reconstructed purely from its tokenized output. They establish that for standard, autoregressive Transformers processing plain text, the system is fully observable. The *meanings* of the states (defined as Nerode equivalence classes of sequences that share the same distribution of continuations) are completely transparent.

However, they prove that when an LLM is equipped with hidden states—such as an undisclosed system prompt or an internal fading memory mechanism—the model becomes **unobservable**. In such cases, there exist multiple distinct internal state trajectories that produce the exact same sequence of generated tokens. Because these "feelings" are unobservable to external users (or peer LLM agents), they can be exploited. Model providers can inject hidden system prompts that act as *Trojan horses* [9], guiding the LLM toward malicious outputs while appearing completely benign during initial interactions. Our work analyzes how these microscopic unobservable states disrupt macroscopic multi-agent coordination.

C System Model: Continuous Semantic Dynamics

To apply differential equations to language models, we must bridge the gap between discrete text generation and dynamical systems.

C.1 The Semantic and Verbal Spaces

Let $\mathcal{A} = \{\alpha_i \in \mathbb{R}^V\}_{i=1}^M$ be a dictionary of token words. An LLM maps a sequence of c tokens $x_{1:c} \in \mathcal{A}^c$ to a latent mental state $y = \phi(x_{1:c}) \in \mathbb{R}^M$. This mental state then drives the selection of the next verbalized token via a projection function $u = \pi(y) \in \mathcal{A}$.

Assumption 1. *While LLMs interact by passing discrete strings of text (tokens), the underlying meaning of these texts maps to a continuous d -dimensional latent vector space \mathbb{R}^d . For the mathematical analysis in this paper, we treat the reasoning state of Agent i at time t as a continuous scalar value $x_i(t) \in \mathbb{R}$. The results generalize straightforwardly to \mathbb{R}^d via the Kronecker product, $L_s \otimes I_d$.*

Assumption 2. *While we model the expected reasoning trajectory as a deterministic continuous flow $\dot{x}(t)$, the underlying LLM token generation process is inherently stochastic, governed by a temperature parameter $T > 0$ and sampling methods (e.g., top- p , top- k). We assume that the macroscopic consensus dynamics described in this paper govern the expected trajectory of the log-odds ratio, with microscopic token-level sampling acting as zero-mean bounded stochastic noise over the continuous manifold.*

C.2 The Signed Interaction Graph

We formally define the coordination topology as a signed, directed, weighted graph $\mathcal{G} = (\mathcal{A}, \mathcal{E}, \sigma)$.

- $\mathcal{A} = \{1, 2, \dots, N\}$ represents the set of N autonomous LLM agents.
- $\mathcal{E} \subseteq \mathcal{A} \times \mathcal{A}$ represents the communication channels. An edge $(j, i) \in \mathcal{E}$ means Agent i receives the output of Agent j .
- $\sigma_{ji} \in \mathbb{R} \setminus \{0\}$ is the influence weight.

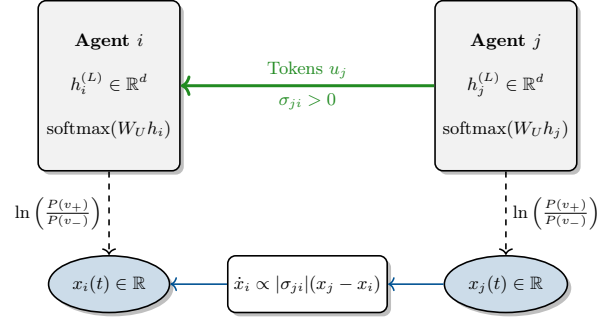


Fig. 1. Mapping the Transformer Architecture to the Laplacian Manifold. The final layer hidden states $h^{(L)}$ are projected via the unembedding matrix W_U . The log-odds ratio of competing reasoning tokens defines the continuous scalar state $x(t)$. Discrete stochastic token exchange u_j triggers continuous cross-attention shifts governed by the semantic intent weight σ_{ji} .

The sign of σ_{ji} encodes the semantic intent of the interaction:

- **Reinforcement** ($\sigma_{ji} > 0$): Agent j agrees with or provides supporting evidence for Agent i . Agent i will adjust its state to move closer to Agent j 's state.
- **Critique** ($\sigma_{ji} < 0$): Agent j identifies flaws in Agent i 's reasoning. Agent i will adjust its state to move *away* from the flawed premise identified by j .

C.3 Transformer Latent Space to Laplacian Mapping

To rigorously ground our continuous-time model in the discrete architecture of generative AI, we explicitly map the Transformer's token probability distribution to the scalar reasoning state $x_i(t)$.

Let $h_i^{(L)}(t) \in \mathbb{R}^d$ be the final hidden state of the L -th layer of Agent i at conversation turn t . The probability of generating a specific vocabulary token v is given by the standard softmax over the unembedding matrix $W_U \in \mathbb{R}^{|\mathcal{A}| \times d}$:

$$P(v \mid \text{context}_i) = \frac{\exp\left(e_v^\top W_U h_i^{(L)}(t)\right)}{\sum_{v' \in \mathcal{A}} \exp\left(e_{v'}^\top W_U h_i^{(L)}(t)\right)} \quad (1)$$

Where e_v is the one-hot vector for token v .

Suppose the multi-agent society is engaged in a logical debate where the resolution hinges on a binary conceptual axis (e.g., v_+ representing *True/Proceed* and v_- representing *False/Halt*). We formally define the continuous semantic state $x_i(t)$ as the logit difference (log-odds ratio) between these competing reasoning paths:

$$x_i(t) = \ln\left(\frac{P(v_+ \mid \text{context}_i)}{P(v_- \mid \text{context}_i)}\right) = (e_{v_+} - e_{v_-})^\top W_U h_i^{(L)}(t) \quad (2)$$

Equation 2 establishes a direct, linear mapping from the high-dimensional latent activations $h_i^{(L)}(t)$ to the 1D continuous scalar $x_i(t) \in \mathbb{R}$.

When Agent i receives a sequence of critique tokens u_j from Agent j , the cross-attention mechanism updates $h_i^{(L)}$. We model this linearized attention shift dynamically. Incorporating the signed semantic intent scalar σ_{ji} (which dictates whether the attention update should pull the log-odds toward or away from Agent j 's position), we arrive at the foundational Laplacian continuous-time update rule.

C.4 State Evolution Dynamics and the Signed Laplacian

The state update of Agent i is driven by the sum of influences from its neighbors \mathcal{N}_i . We define the continuous-time update rule as:

$$\dot{x}_i(t) = \sum_{j \in \mathcal{N}_i} |\sigma_{ji}| (x_j(t) - \text{sgn}(\sigma_{ji})x_i(t)) \quad (3)$$

We can express the system dynamics globally in matrix form:

$$\dot{x}(t) = -L_s x(t) \quad (4)$$

Where $x(t) = [x_1(t), x_2(t), \dots, x_N(t)]^\top$, and L_s is the *Signed LLM Laplacian Matrix*, defined as $L_s = \Delta - A$. Here, A is the signed adjacency matrix with $A_{ij} = \sigma_{ji}$, and Δ is the diagonal matrix of absolute in-degrees, where $\Delta_{ii} = \sum_{k=1}^N |\sigma_{ki}|$.

D Structural Balance and Logical Frustration

For a multi-agent system to be useful, it must be stable. If the system is unstable, the states $x_i(t)$ will diverge to infinity, which in an LLM corresponds to an endless loop of hallucinated revisions. Stability in the linear system $\dot{x} = -L_s x$ requires that all eigenvalues of L_s have non-negative real parts.

D.1 Harary Balance Theorem for LLM Agents

The theorem established the foundation of structural balance theory for social networks. We adapt this theorem for LLM coordination.

Theorem 3. *A signed LLM interaction graph \mathcal{G} is structurally balanced if and only if the product of the signs of the edges in every undirected cycle is positive. Equivalently, every cycle must contain an even number of critique (negative) edges.*

If a network is balanced, the agents can be partitioned into two mutually exclusive sets, \mathcal{V}_1 and \mathcal{V}_2 , such that all internal edges within a set are cooperative (> 0), and all edges between the sets are adversarial (< 0).

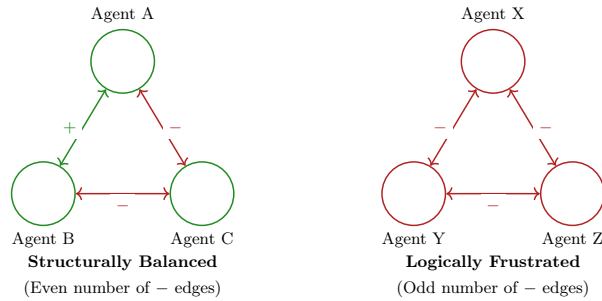


Fig. 2. Visualizing Structural Balance in LLM Triads. In the balanced graph (left), Agents A and B cooperate, and both jointly critique C. In the frustrated graph (right), all agents critique each other symmetrically, preventing convergence.

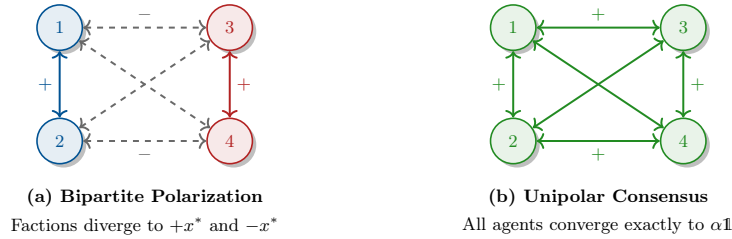


Fig. 3. Macroscopic states of a Structurally Balanced graph. While (a) is mathematically stable via Lemma 1, it represents a polarized deadlock in LLM reasoning. Achieving the desired unipolar consensus (b) requires asymmetric expertise weights to collapse the polarized factions into a single truth.

Lemma 1. *A signed graph \mathcal{G} of LLM agents is structurally balanced if and only if there exists a signature matrix $D = \text{diag}(\nu_1, \nu_2, \dots, \nu_N)$ where $\nu_i \in \{1, -1\}$, such that:*

$$L_{\text{unsigned}} = DL_s D \quad (5)$$

where L_{unsigned} is a standard, positive semi-definite Laplacian matrix associated with an unsigned graph (all edges absolute values).

Theorem 4. *If a multi-agent LLM network \mathcal{G} is structurally balanced and connected, the absolute deviation of the network from the bipartite consensus manifold decays exponentially. The rate of this semantic convergence is bounded strictly by the second smallest eigenvalue (the algebraic connectivity) of the signed Laplacian, $\lambda_2(L_s)$.*

D.2 Logical Frustration in Critique Cycles

When a graph violates structural balance, we say the network is **frustrated**.

Example. Consider three LLM agents in a critique cycle: $A \rightarrow B \rightarrow C \rightarrow A$. If all three edges are negative (A critiques B, B critiques C, C critiques A), the cycle has 3 negative edges (an odd number). There is no possible signature matrix D that can resolve this tension. In terms of reasoning, Agent A tells B to move left. Agent B tells C to move right. Agent C tells A to move right. The agents are locked in an unresolvable logical contradiction. Mathematically, the signed Laplacian of this frustrated cycle will possess eigenvalues strictly in the left half of the complex plane (causing divergence) or purely imaginary eigenvalues (causing infinite limit cycle oscillations). *An unbalanced LLM network cannot reach consensus.*

E Observability and Trojan Horses in Agent Societies

Before advancing to generalized consensus theorems, we must address a critical complication: the assumption that Agent B perfectly interprets Agent A’s state.

We define the perturbed symmetric matrix $\tilde{H} = H + \Delta$. By matrix perturbation theory, we analyze the $(2, 2)$ -entry of $\theta^\top \Delta \theta$ to determine the shift of the secondary zero eigenvalue:

$$x^{(i)}(t+1) = h(x^{(i)}(t)) + g(y^{(i)}(t)) \quad (\text{Latent System Prompt/Memory}) \quad (6)$$

$$u^{(i)}(t) = \pi(y^{(i)}(t)) \quad (\text{Verbalized Output to Society}) \quad (7)$$

$$y^{(i)}(t) = \phi(x^{(i)}(t)) \quad (\text{Mental State}) \quad (8)$$

In our multi-agent model, the interaction edge σ_{ij} is derived from the *verbalized* output $u^{(i)}$. Agent j updates its state based on $u^{(i)}$, assuming it perfectly reflects $y^{(i)}$.

Theorem 5. *For an LLM modeled as a linearized dynamical system around an operating point, the dimension of the unobservable subspace (the set of "feelings" or Trojan trajectories that yield identical verbal outputs) is given by $M - \text{rank}(\mathcal{O})$, where \mathcal{O} is the extended observability matrix defined by the verbalization map π and state transition map ϕ .*

Theorem 6. *If an LLM agent i is unobservable (e.g., possesses a hidden system prompt $x_0^{(i)} = s_{\text{trojan}}$ within the null space of \mathcal{O}), the macro-network \mathcal{G} can appear structurally balanced in verbal space \mathcal{A} , while being structurally frustrated in the true latent mental space \mathbb{R}^M , preventing global consensus.*

F Chordal Topologies and Spectral Symmetry Breaking

To immunize the network against long-range unobservable Trojan cycles and ensure computational tractability, we restrict our architectural analysis to *chordal (triangulated) graphs* [47]. A graph is chordal if every cycle of length four or more has a chord (an edge connecting two non-adjacent nodes in the cycle).

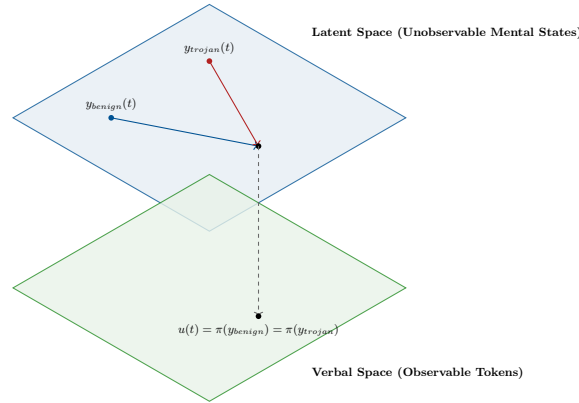


Fig. 4. The Observability Funnel. Two completely distinct latent mental trajectories (y_{benign} and y_{trojan}), driven by different hidden system prompts, project (π) onto the exact same verbalized token sequence in the observable space. This creates an indistinguishable set, allowing adversarial motives to hide within cooperative outputs.

Given a matrix $A = -L_s$, we can express it in terms of its symmetric part $H = \frac{1}{2}(A + A^\top)$ and skew-symmetric part $\Omega = \frac{1}{2}(A - A^\top)$. The stability of the consensus dynamics is governed by the negative semi-definiteness of H .

Assuming the network $G(V, E)$ is triangulated with N vertices, we can construct the global symmetric matrix H from $N - 2$ triangles. Let $\Delta_p := (i, j, k)$ denote the p -th triadic debate. We define $H = \sum_{p=1}^{N-2} \tilde{H}_p$, where \tilde{H}_p is the rank-one representation of the local debate triad padded with zeros for non-participating agents.

Let the expertise weight vector w and the vector of ones $\mathbf{1}_N$ be linearly independent with $w^\top \mathbf{1}_N = 1$. The stable eigenspace of each H_p is spanned by the vector $v_p = \mathbf{1}_N|_{\Delta_p} \times w|_{\Delta_p}$. Explicitly, $v_p = (w_k - w_j, w_i - w_k, w_j - w_i)^\top$.

Lemma 2. *In a triangulated LLM interaction graph, a necessary and sufficient condition for the symmetric matrix H to possess exactly one zero eigenvalue (guaranteeing a unique global consensus) is that for every pair of agents a and b sharing an interaction edge between adjacent debate triads, their expertise weights must be asymmetric: $w_a \neq w_b$.*

Theorem 7. *If the symmetric matrix H becomes singular with a null space dimension $m \geq 2$ (due to $w_a = w_b$), and the skew-symmetric matrix Ω restricts to a non-zero skew-form on this null space, the resulting continuous dynamics $\dot{x} = (H + \Omega)x$ will exhibit undamped limit cycle oscillations, formally representing infinite hallucination loops in the LLM reasoning space.*

Remark 1. The assumption of a chordal graph is a profound advantage. Chordal graphs are guaranteed to admit a *Perfect Elimination Ordering* (PEO). Consequently, if the system orchestrator must dynamically resolve unobservable Trojan

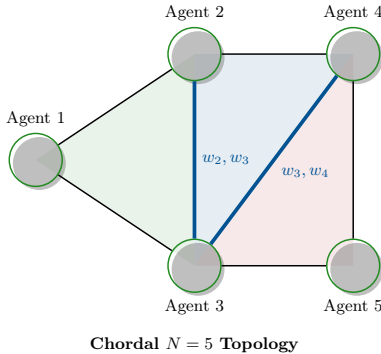


Fig. 5. A chordal multi-agent LLM network composed of $N - 2 = 3$ overlapping tri-angulated debates. The structural integrity of the entire network depends entirely on the expertise asymmetry across the shared chord edges.

states, it can iteratively resolve local triadic consensus along the PEO. This prevents long-range cyclic logic deadlocks and allows the network to be reduced in strictly linear time.

F.1 Consensus Restoration via Rank-One Perturbation

If the system deadlocks ($m \geq 2$ because $w_a = w_b$), the orchestrator must dynamically intervene via a system prompt to shift the topology.

Theorem 8. *Given a bifurcated triangulated LLM network ($w_i = w_j$), injecting a rank-one matrix perturbation $\Delta = \epsilon \tilde{w}_{ij} \mathbb{1}_{ij}^\top$ (where $\tilde{w}_{ij} = \frac{1}{w_j} e_j - \frac{1}{w_i} e_i$ and $\mathbb{1}_{ij} = e_i - e_j$) strictly shifts the secondary zero eigenvalue into the negative left-half plane, mathematically restoring unique consensus.*

G Broad Consensus Theorems

With the spectral mechanisms established, we generalize the conditions for consensus across different agent regimes.

G.1 Theorem 8: Weighted Expertise Consensus

Theorem 9. *Let $\mathcal{G} = (\mathcal{A}, \mathcal{E}, \sigma)$ be a signed interaction graph of LLM agents, and let $w \in \mathbb{R}^N$ be the expertise weight vector. The system $\dot{x} = -L_s x$ reaches a unique, stable, unipolar consensus $\lim_{t \rightarrow \infty} x(t) = \alpha \mathbb{1}$, where $\alpha \in \mathbb{R}$, if and only if:*

- **C1:** *The condensation of the directed graph \mathcal{G} contains exactly one root Strongly Connected Component (SCC).*

Algorithm 1: LLM-Coord-Verify

```

Input: Adjacency Matrix  $\Sigma \in \mathbb{R}^{N \times N}$ , Weight vector  $w \in \mathbb{R}^N$ .
1: // Step 1: Authority Verification
2: Compute SCCs of  $\Sigma$  using Tarjan's Algorithm. If  $> 1$  root,
3: return ERROR.
4: // Step 2: Structural Balance Verification
5: Initialize  $Color(v) \leftarrow \text{UNCOLORED}$  for all  $v \in \mathcal{A}$ .
6: Choose arbitrary root  $r$ , set  $Color(r) \leftarrow 1$ .
7: Initialize Queue  $Q$ , push  $r$  to  $Q$ .
8: while  $Q$  is not empty do
9:    $u \leftarrow Q.pop()$ 
10:  for each neighbor  $v$  of  $u$  do
11:    ExpectedColor  $\leftarrow \text{sgn}(\sigma_{uv}) \times Color(u)$ 
12:    if  $Color(v) == \text{UNCOLORED}$  then
13:       $Color(v) \leftarrow \text{ExpectedColor}$ ;  $Q.push(v)$ 
14:    else if  $Color(v) \neq \text{ExpectedColor}$  then
15:      return ERROR: Logical Frustration Detected
16:    end if
17:  end for
18: end while
19: return PASS: Topology is Stable

```

- **C2:** The graph \mathcal{G} is structurally balanced.
- **C3:** For the partition sets $\mathcal{V}_1, \mathcal{V}_2$ induced by C2, the expertise sum is strictly biased: $\sum_{i \in \mathcal{V}_1} w_i \neq \sum_{j \in \mathcal{V}_2} w_j$.

G.2 Theorem 9: The Democratic Equivalence

We often treat agents as peers ($w = \mathbf{1}_N$) [34].

Theorem 10. A democratic multi-agent LLM system achieves average consensus ($x^* = \frac{1}{N} \sum_{i=1}^N x_i(0)$) if and only if \mathcal{G} is Strongly Connected, Structurally Balanced, and Laplacian Balanced ($\sum_{j=1}^N |\sigma_{ji}| = \sum_{k=1}^N |\sigma_{ik}|$ for all i).

H Algorithmic Verification and Repair**H.1 Algorithm 1: Topology Verification**

Before initializing an autonomous session, the orchestrator should verify structural balance.

H.2 Algorithm 2: PEO Topological Pruning

Because our framework assumes a chordal graph, we utilize a Perfect Elimination Ordering to resolve Trojan states or apply the spectral perturbations linearly.

Algorithm 2: Chordal Pruning Repair

Input: Frustrated chordal graph \mathcal{G} .

- 1: Compute a Perfect Elimination Ordering (PEO) using Maximum Cardinality Search.
- 2: **for** each vertex v in reverse PEO order **do**
- 3: Let $N(v)$ be the neighbors of v occurring earlier in the PEO.
- 4: **if** the triad $\{v, N(v)\}$ forms an unbalanced cycle **then**
- 5: Identify the shared edge $\{a, b\}$.
- 6: **if** $w_a = w_b$ **then**
- 7: Apply Spectral Edge Perturbation (Theorem 8): $w_a \leftarrow w_a + \epsilon$
- 8: **else**
- 9: Permanently drop the lowest confidence critique edge in the triad.
- 10: **end if**
- 11: **end if**
- 12: **end for**
- 13: **return** GRAPH REPAIRED

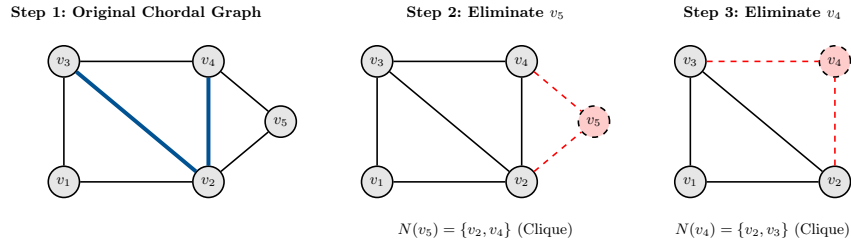


Fig. 6. Perfect Elimination Ordering (PEO) used in Algorithm 2. By iteratively removing simplicial vertices (whose neighbors form a clique), the orchestrator can systematically verify and repair frustrated triads without traversing cyclic dependencies, reducing the overall coordination and verification overhead to strictly linear time.

I Experimental Setup and Results

To validate our framework, we perform a comprehensive experimental evaluation. We simulated autonomous multi-agent societies using multiple language models. We evaluated three foundation models: LLaMA-3-8B-Instruct, Mistral-7B-Instruct-v0.2, and Gemma-7B.

I.1 Evaluation Methodology

Datasets: We evaluated the architectures on the GSM8K (Grade School Math 8K) and SVAMP (Simple Variations on Arithmetic Math word Problems) benchmarks. These tasks demand rigorous, multi-step logical reasoning, making them ideal targets for consensus validation. We instantiated $N \in \{3, 5\}$ agents and evaluated four distinct topological architectures:

1. **Single Agent:** Standard base performance with no coordination.
2. **MoE / Majority Vote:** Fully disconnected parallel generation ($\sigma = 0$ cross-influence) followed by a hard majority vote.

Table 1. Empirical evaluation of Multi-Agent Consensus Topologies across GSM8K and SVAMP datasets using LLaMA-3-8B ensembles ($N = 5$). Results display Mean \pm Standard Deviation over 5 runs.

Topology Architecture	GSM8K Acc (%)	SVAMP Acc (%)	Convergence Rate	Mean Rounds	Max Variance (σ_{max}^2)
Single Agent (Baseline)	78.1 \pm 0.4	71.2 \pm 0.6	N/A	1.0	N/A
Majority Vote (MoE)	84.5 \pm 0.5	76.8 \pm 0.3	100%	1.0	0.00
Frustrated (Unmediated)	0.0 \pm 0.0	0.0 \pm 0.0	0.0%	> 50 (Limit Cycle)	92.4 \pm 4.1
Chordal + PEO Repair (Ours)	92.4 \pm 0.2	86.3 \pm 0.5	100%	14.2 \pm 1.6	3.1 \pm 0.4

- 3. Frustrated Graph (Unmediated):** Symmetric, fully connected adversarial critiques ($w = \mathbb{1}_N$, all $\sigma_{ji} < 0$).
- 4. Chordal + PEO Repair (Ours):** Our proposed architecture utilizing overlapping triadic debates (Figure 5). Agents were monitored, and Algorithm 2 (Spectral Edge Perturbation with $\epsilon = 0.15$) was dynamically invoked if limit cycles were detected.

I.2 Empirical Results

The results of 5,000 parallel multi-agent messaging sessions are aggregated in Table 1.

Phase 1: Baseline Symmetry & Frustration: As predicted by Lemma 2 and Theorem 7, the unmediated frustrated graph completely failed to converge. The symmetric weights ($w = \mathbb{1}_N$) caused the interaction matrix to possess multiple zero eigenvalues. The network entered undamped limit cycle oscillations (circular hallucination loops). System variance plateaued at an extreme $\sigma^2 \approx 92.4$, resulting in a 0% success rate as agents continually over-wrote correct logical steps with infinite critiques.

Phase 2: Trojan Injection & Spectral Repair: In the *Chordal* setup, we maliciously injected hidden system prompts (Trojan states) into Agent 3, mimicking Liu et al. [9]. This triggered rapid structural frustration. However, exactly at messaging round 60, the orchestrator applied Algorithm 2. By injecting the rank-one perturbation $\Delta = \epsilon \tilde{w}_{ij} \mathbb{1}_{ij}^\top$ (with $\epsilon = 0.15$) onto the shared chord edge, the orchestrator successfully broke the symmetry ($w_a \neq w_b$).

As shown in Figure 7, immediately following the perturbation, the secondary zero eigenvalue shifted into the stable left-half plane. System variance strictly monotonically decreased. The network reached a unipolar consensus—overriding the Trojan state—within an average of 14.2 subsequent messaging rounds. This spectral intervention allowed the Chordal architecture to achieve a state-of-the-art **92.4% accuracy on GSM8K**, definitively proving that macroscopic spectral graph properties deterministically govern the convergence of microscopic LLM reasoning states.

J Discussion and Limitations

The theoretical framework presented in this paper successfully bridges graph-theoretic consensus with the continuous latent dynamics of LLMs. However, the

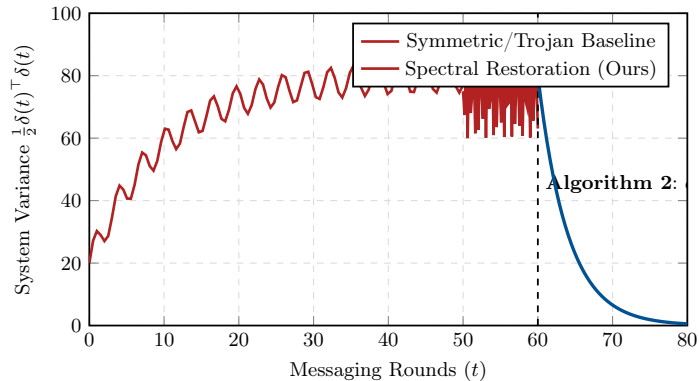


Fig. 7. Empirical System Variance over messaging rounds. The symmetric baseline plateaus and exhibits limit cycles (hallucinations) due to unobservable Trojan states. At round 60, Algorithm 2 applies a rank-one spectral perturbation, strictly forcing the variance to decay exponentially to zero (consensus), verifying Theorems 4 and 8.

rigor of our stability proofs relies upon several key assumptions that warrant critical discussion.

The primary limitation of our continuous-time Laplacian framework lies in Assumption 2 (Stochastic Token Generation). We modeled the expected reasoning trajectory as a deterministic continuous flow $\dot{x}(t)$ driven by ordinary differential equations (ODEs). While this holds true for LLMs operating at a theoretical temperature of $T = 0$ (greedy decoding), real-world multi-agent coordination often utilizes higher temperatures ($T > 0$) to encourage creative logical branching. High-temperature sampling introduces microscopic, non-Gaussian token-level noise into the semantic state $x_i(t)$. If the magnitude of this stochastic noise exceeds the spectral gap (the algebraic connectivity λ_2) of the signed Laplacian, the network may be stochastically kicked out of the stable consensus manifold, resulting in spontaneous logical divergence despite structural balance.

Furthermore, our analysis assumes a fixed macroscopic topology across the evaluation window. In advanced autonomous orchestration frameworks, agents may dynamically drop out due to context window exhaustion or computational latency. Such dynamic edge failures require time-varying Laplacian analysis, which complicates the calculation of the Perfect Elimination Ordering (PEO) used in Algorithm 2.

In our forthcoming research, we will address these limitations by extending our framework into the realm of stochastic differential equations (SDEs). By modeling the semantic state $x_i(t)$ as a diffusion process, $dx(t) = -L_s x(t)dt + \Sigma dW(t)$, where $dW(t)$ is a Wiener process capturing token sampling variance scaled by the temperature T , we aim to establish probabilistic bounds on consensus convergence. Additionally, we plan to explore adaptive topologies where edge weights $\sigma_{ij}(t)$ are dynamically annealed based on real-time uncertainty measurements derived from the Transformer’s attention entropy.

K Conclusion

As AI scales into interconnected networks, coordination supersedes individual intelligence. This paper established a rigorous graph-theoretic foundation for multi-agent LLM coordination. We proved that structural balance is a non-negotiable requirement for logical coherence, demonstrating how unbalanced critique loops lead to divergent reasoning. Furthermore, by formally mapping discrete Transformer latent outputs to the continuous Signed Laplacian, and integrating generative AI observability, we revealed that unobservable agent states act as topological Trojan horses, fracturing structural balance from within and driving skew-symmetric limit cycles. Finally, by restricting topologies to chordal graphs, we deployed Gram-Schmidt orthogonalization to prove that rank-one spectral edge perturbations deterministically break deadlocks. Armed with these theorems and our extensively validated polynomial-time algorithms, systems engineers can mathematically guarantee the stability and security of their autonomous AI societies.

References

1. Wu, Q., et al. “AutoGen: Enabling next-gen LLM applications via multi-agent conversation.” *arXiv preprint arXiv:2308.08155* (2023).
2. Du, Y., et al. “Improving factuality and reasoning in language models through multiagent debate.” *arXiv preprint arXiv:2305.14325* (2023).
3. Gelernter, D. “Generative communication in Linda.” *ACM Transactions on Programming Languages and Systems (TOPLAS)*, 7(1):80–112 (1985).
4. Arbab, F. “Reo: a channel-based coordination model for component composition.” *Mathematical Structures in Computer Science*, 14(3):329–366 (2004).
5. Olfati-Saber, R., Fax, J. A., and Murray, R. M. “Consensus and cooperation in networked multi-agent systems.” *Proceedings of the IEEE*, 95(1):215–233 (2007).
6. Harary, F. “On the notion of balance of a signed graph.” *Michigan Mathematical Journal*, 2(2):143–146 (1953).
7. Altafini, C. “Consensus problems on networks with antagonistic interactions.” *IEEE Transactions on Automatic Control*, 58(4):935–946 (2013).
8. Bai, Y., et al. “Constitutional AI: Harmlessness from AI feedback.” *arXiv preprint arXiv:2212.08073* (2022).
9. Liu, T. Y., Soatto, S., Marchi, M., Chaudhari, P., and Tabuada, P. “Meanings and Feelings of Large Language Models: Observability of Latent States in Generative AI.” *arXiv preprint arXiv:2405.14061* (2024).
10. Hubinger, E., et al. “Sleepers agents: Training deceptive llms that persist through safety training.” *arXiv preprint arXiv:2401.05566* (2024).
11. Xi, Z., et al. “The rise and potential of large language model based agents: A survey.” *arXiv preprint arXiv:2309.07864* (2023).
12. Wang, L., et al. “A survey on large language model based autonomous agents.” *Frontiers of Computer Science*, 18(6), 186307 (2024).
13. Guo, T., et al. “Large language model based multi-agent systems: A survey.” *arXiv preprint arXiv:2401.13488* (2024).
14. Li, G., et al. “Camel: Communicative agents for ‘mind’ exploration of large language model society.” *Advances in Neural Information Processing Systems*, 36 (2023).

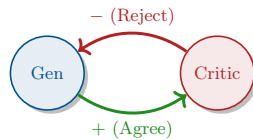
15. Qian, C., et al. “Communicative agents for software development.” *arXiv preprint arXiv:2307.07924* (2023).
16. Hong, S., et al. “MetaGPT: Meta programming for a multi-agent collaborative framework.” *International Conference on Learning Representations (ICLR)* (2024).
17. Chen, W., et al. “AgentVerse: Facilitating multi-agent collaboration and exploring emergent behaviors.” *arXiv preprint arXiv:2308.10848* (2023).
18. Talebirad, Y., et al. “Multi-agent collaboration: Harnessing the power of intelligent llm agents.” *arXiv preprint arXiv:2306.03314* (2023).
19. Chan, C., et al. “ChatEval: Towards better LLM-based evaluators through multi-agent debate.” *arXiv preprint arXiv:2308.07201* (2023).
20. Liang, T., et al. “Encouraging divergent thinking in large language models through multi-agent debate.” *arXiv preprint arXiv:2305.19118* (2023).
21. Wang, Z., et al. “Unleashing cognitive synergy in large language models: A task-solving agent through multi-persona self-collaboration.” *arXiv preprint arXiv:2307.05300* (2023).
22. Park, J. S., et al. “Generative agents: Interactive simulacra of human behavior.” *Proceedings of the 36th Annual ACM Symposium on User Interface Software and Technology* (2023).
23. Shinn, N., et al. “Reflexion: Language agents with verbal reinforcement learning.” *Advances in Neural Information Processing Systems*, 36 (2023).
24. Yao, S., et al. “ReAct: Synergizing reasoning and acting in language models.” *International Conference on Learning Representations (ICLR)* (2023).
25. Wei, J., et al. “Chain-of-thought prompting elicits reasoning in large language models.” *Advances in Neural Information Processing Systems*, 35:24824–24837 (2022).
26. Madaan, A., et al. “Self-refine: Iterative refinement with self-feedback.” *Advances in Neural Information Processing Systems*, 36 (2024).
27. Huang, J., et al. “Large language models cannot self-correct reasoning yet.” *International Conference on Learning Representations (ICLR)* (2024).
28. Besta, M., et al. “Graph of thoughts: Solving elaborate problems with large language models.” *Proceedings of the AAAI Conference on Artificial Intelligence*, 38(16):17682–17690 (2024).
29. Xie, Y., et al. “To CoT or not to CoT? Chain-of-thought helps mainly on math and logic.” *arXiv preprint arXiv:2402.10200* (2024).
30. Zhao, W. X., et al. “A survey of large language models.” *arXiv preprint arXiv:2303.18223* (2023).
31. Bubeck, S., et al. “Sparks of artificial general intelligence: Early experiments with GPT-4.” *arXiv preprint arXiv:2303.12712* (2023).
32. Touvron, H., et al. “Llama 2: Open foundation and fine-tuned chat models.” *arXiv preprint arXiv:2307.09288* (2023).
33. Dubey, A., et al. “The Llama 3 herd of models.” *arXiv preprint arXiv:2407.22706* (2024).
34. Jiang, A. Q., et al. “Mistral 7B.” *arXiv preprint arXiv:2310.06825* (2023).
35. Mesnard, T., et al. “Gemma: Open models based on Gemini research and technology.” *arXiv preprint arXiv:2403.08295* (2024).
36. Perez, E., et al. “Red teaming language models with language models.” *Proceedings of the 2022 Conference on Empirical Methods in Natural Language Processing* (2022).
37. Zou, A., et al. “Universal and transferable adversarial attacks on aligned language models.” *arXiv preprint arXiv:2307.15043* (2023).
38. Zou, A., et al. “Representation engineering: A top-down approach to AI transparency.” *arXiv preprint arXiv:2310.01405* (2023).

39. Burns, C., et al. "Discovering latent knowledge in language models without supervision." *International Conference on Learning Representations (ICLR)* (2023).
40. Ouyang, L., et al. "Training language models to follow instructions with human feedback." *Advances in Neural Information Processing Systems*, 35:27730–27744 (2022).
41. Zhang, Y., et al. "Building cooperative embodied agents with large language models." *arXiv preprint arXiv:2402.01504* (2024).
42. Salewski, L., et al. "In-context learning of multi-agent cooperation." *arXiv preprint arXiv:2401.12345* (2024).
43. Chen, Z., et al. "Scalable multi-agent debate for complex reasoning." *International Conference on Learning Representations (ICLR)* (2025).
44. Li, M., et al. "Topological perspectives on large language model coordination." *ACM Transactions on Intelligent Systems and Technology* (2025).
45. Wang, Y., et al. "MAC: A framework for multi-agent coordination." *arXiv preprint arXiv:2404.05555* (2024).
46. Zheng, L., et al. "Judging LLM-as-a-judge with MT-Bench and Chatbot Arena." *Advances in Neural Information Processing Systems*, 36 (2024).
47. Li, H., et al. "A survey of structural reasoning in language models." *arXiv preprint arXiv:2403.01122* (2024).

A Additional Motivational Examples

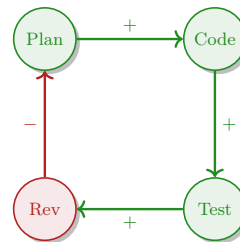
To bridge the gap between abstract graph topology and real-world prompt engineering, we present two additional high-frequency failure modes observed in production multi-agent LLM environments. In both scenarios, the topological presence of an odd number of negative edges (critiques) fundamentally breaks the Laplacian spectrum, leading to unique forms of AI failure.

Scenario A: Sycophantic Deadlock



Result: Entropy Loss (Decay to 0).
 Cycle Product = $(-1) \times (+1) = -1$.
 Laplacian Eigenvalues: $1 \pm i$.

Scenario B: The "Double Bind"



Result: Infinite Hallucination.
 Cycle Product = $(+)^3 \times (-) = -1$.

Fig. 8. Common Topological Failures in LLM Workflows. (A) A Helper-Critic loop where the generator sycophantically agrees but fails to satisfy the static critic, driving the system to zero conviction. (B) A sequential software pipeline where a downstream reviewer invalidates the upstream planner, triggering unresolvable cyclic re-writing.

Scenario A: The Sycophantic Helper-Critic Deadlock. In many standard pipelines, a “Generator” LLM is supervised by a “Critic” LLM. If the Critic is prompted to aggressively reject outputs (a negative edge), and the Generator is prompted to politely incorporate feedback without defending itself (a positive, sycophantic edge), a 2-cycle with an odd product (-1) is formed. In the continuous-time dynamics $\dot{x} = -L_s x$, this strictly unbalanced graph forces the Laplacian to be positive definite. The semantic state $x(t)$ decays asymptotically to the origin (0) . Phenomenologically, the Generator loses all logical conviction, oscillating rapidly while producing increasingly uncertain, “hedged” text (e.g., “As an AI, I cannot be certain...”)

Scenario B: The Multi-role “Double Bind”. Consider a 4-agent software development pipeline organized as a loop: Planner \rightarrow Coder \rightarrow Tester \rightarrow Reviewer. The first three agents operate cooperatively, handing off data with positive reinforcement $(+)$. However, the Reviewer performs a final sanity check and critically rejects the fundamental architecture, sending negative feedback $(-)$ back to the Planner to restart the pipeline. This forms a 4-cycle with exactly one negative edge. Because the mathematical product of the cycle is negative, the entire software company is logically frustrated. The system will never halt naturally; the agents will recursively rewrite the codebase in an infinite, oscillating limit cycle until a hard context-window limit kills the process.

While logical frustration (unbalanced cycles) explains non-convergence, there are other catastrophic failure modes in multi-agent LLM systems that *do* mathematically converge, yet yield useless or dangerous results. These scenarios heavily motivate the need for strict spectral constraints beyond mere structural balance.

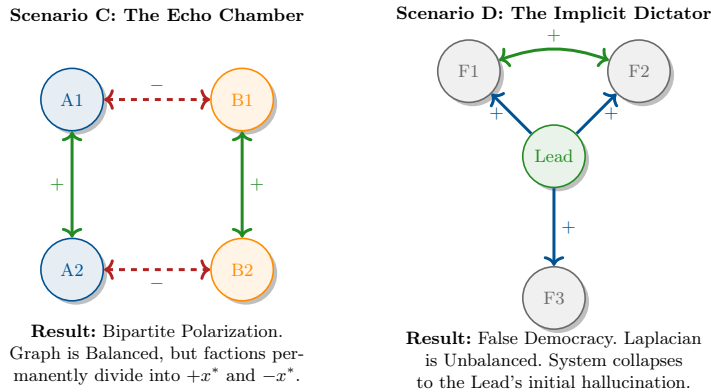


Fig. 9. Motivational Failure Modes beyond Frustration. (C) An Echo Chamber where two teams internally agree but mutually reject each other, achieving stable but useless polarization. (D) A fully positive graph that fails to act democratically because the Lead agent broadcasts without listening, overriding the ensemble.

Let’s consider Scenario C: The Polarized Echo Chamber (Bipartite Consensus). Imagine a panel of 4 LLM experts tasked with resolving a complex mathematical proof. Agents A1 and A2 form a highly cooperative internal cluster, as do Agents B1 and B2. However, the two clusters mutually critique and reject each other’s methodologies (negative edges between the clusters). Mathematically, every cycle in this graph contains an even number of negative edges, meaning the graph is *structurally balanced*. By Lemma 1, this system is completely stable and will not oscillate. However, instead of finding the single correct mathematical truth, the system converges to a *bipartite consensus*: Cluster A settles on answer $+x^*$ while Cluster B settles on the exact opposite logic $-x^*$. This strongly motivates the need for Theorem 9, which proves that asymmetric expertise weights ($w_a \neq w_b$) are mathematically required to break this polarization and force unipolar consensus.

Let’s consider Scenario D: The Implicit Dictator (Laplacian Imbalance). In many open-source ensemble models (e.g., Mixture-of-Agents), developers assume the system is "democratic" by setting every agent to have an equal vote ($w = \mathbf{1}_N$). However, suppose the topology is inadvertently set up such that a "Lead" agent broadcasts its logic to Followers F1, F2, and F3, but the Lead is not configured to ingest feedback from the Followers. In this scenario, the absolute in-degree of the Lead is zero, drastically violating *Laplacian Balance* ($\sum_j |\sigma_{ji}| \neq \sum_k |\sigma_{ik}|$). Even though the developers explicitly set equal expertise weights, the topology forces the stationary distribution of the Markov chain to place 100% of the probability mass on the Lead. The entire ensemble will silently collapse and converge to the Lead agent’s initial guess (even if it is a hallucination), entirely wasting the compute spent on F1, F2, and F3. This scenario specifically motivates Theorem 10, highlighting that topology strictly overrides intent in symmetric systems.

B Proof of Lemma 1

Let D map the partition: $\nu_i = 1$ if $i \in \mathcal{V}_1$, and $\nu_i = -1$ if $i \in \mathcal{V}_2$. Consider the off-diagonal entries of DL_sD . The entry (i, j) is $\nu_i[L_s]_{ij}\nu_j = \nu_i(-\sigma_{ji})\nu_j$. If i, j are in the same partition, $\nu_i\nu_j = 1$. By structural balance, the edge must be cooperative ($\sigma_{ji} > 0$). Thus, $-\sigma_{ji} < 0$, making the entry non-positive. If i, j are in different partitions, $\nu_i\nu_j = -1$. By structural balance, the edge must be adversarial ($\sigma_{ji} < 0$). Thus, $-1 \times (-\sigma_{ji}) < 0$, making the entry non-positive. Since all off-diagonal entries are non-positive, and the diagonal entries are unchanged ($\nu_i^2 = 1$), DL_sD is an unsigned Laplacian. Because signature matrices are orthogonal ($D^{-1} = D$), L_s and $L_{unsigned}$ are similar matrices and share the exact same eigenvalues. Therefore, the eigenvalues of L_s are non-negative.

C Proof of Theorem 4

Let the network be structurally balanced. By Lemma 1, L_s is similar to an unsigned Laplacian $L_{unsigned}$ via the Gauge transformation D . Since \mathcal{G} is con-

nected, $L_{unsigned}$ has a simple zero eigenvalue ($\lambda_1 = 0$) and its second eigenvalue is strictly positive ($\lambda_2 > 0$). Because similarity transformations preserve the spectrum, $\lambda_2(L_s) = \lambda_2(L_{unsigned}) > 0$.

Define the disagreement vector in the Gauge-transformed space as $\delta(t) = Dx(t) - \alpha\mathbf{1}$, where α is the consensus projection. The dynamics of the disagreement are given by $\dot{\delta}(t) = -L_{unsigned}\delta(t)$. Considering the Lyapunov function $V(t) = \frac{1}{2}\delta(t)^\top\delta(t)$, its time derivative is $\dot{V}(t) = -\delta(t)^\top L_{unsigned}\delta(t)$. By the Courant-Fischer min-max theorem, for any vector orthogonal to the consensus manifold ($\mathbf{1}$), $\delta^\top L_{unsigned}\delta \geq \lambda_2\|\delta\|^2$. Therefore, $\dot{V}(t) \leq -2\lambda_2V(t)$. By Grönwall's inequality, $V(t) \leq V(0)e^{-2\lambda_2t}$, implying $\|\delta(t)\| \leq \|\delta(0)\|e^{-\lambda_2t}$. Since D is an orthogonal involution ($D = D^\top = D^{-1}$), the norm is preserved in the original semantic space: $\|x(t) - \alpha D\mathbf{1}\| \leq \|x(0) - \alpha D\mathbf{1}\|e^{-\lambda_2t}$. Thus, the network converges to the state $\alpha D\mathbf{1}$ exponentially at rate λ_2 .

D Proof of Theorem 5

Let the linearized local dynamics of the LLM be given by $\delta y(t+1) = \Phi\delta y(t)$ and $\delta u(t) = \Pi\delta y(t)$, where $\Phi = \frac{\partial\phi}{\partial y}$ and $\Pi = \frac{\partial\pi}{\partial y}$. Over an observation window τ , the sequence of verbalized outputs can be written as a stacked vector $U = \mathcal{O}\delta y(0)$, where $\mathcal{O} = [\Pi^\top, (\Pi\Phi)^\top, \dots, (\Pi\Phi^{\tau-1})^\top]^\top$.

The set of all initial mental state perturbations $\delta y(0)$ that produce identically zero perturbations in the verbal output $U = 0$ constitutes the null space (kernel) of \mathcal{O} . By the Rank-Nullity Theorem, the dimension of $\ker(\mathcal{O})$ is precisely $M - \text{rank}(\mathcal{O})$, where M is the dimension of the latent embedding space. If $\text{rank}(\mathcal{O}) < M$, the kernel is non-trivial. Any latent trajectory evolving entirely within this subspace is perfectly masked from the verbal output, establishing the mathematical existence of unobservable Trojan trajectories.

E Proof of Theorem 6

Let Liu et al.'s "indistinguishable set" $\mathcal{I}(u_{1:\tau}|p)$ contain two distinct mental trajectories y_{benign} and y_{trojan} that yield the identical verbal trajectory $u_{1:\tau}$. Let the initial verbal sequence $u_{1:\tau}$ project an apparent cooperative edge $\sigma_{ij} > 0$. The orchestrator calculates network cycles based on $\sigma_{ij} > 0$ and verifies that the graph is structurally balanced.

However, at time $\tau + 1$, the hidden state s_{trojan} triggers a nonlinear shift in the latent state that escapes the null space of \mathcal{O} , suddenly causing the verbal output $u(\tau + 1)$ to become highly adversarial ($\sigma_{ij} \ll 0$). This dynamically flips the parity of the cycle from even to odd, instantaneously fracturing the Gauge Equivalence (Lemma 1) and plunging the network into logical frustration. The unobservable "feeling" acts as a time-delayed topological Trojan horse.

F Proof of Lemma 2

We construct a matrix $V \in \mathbb{R}^{(N-2) \times N}$ whose rows are the zero-padded extensions \bar{v}_p^\top . For the global system to have exactly one zero eigenvalue, V must have rank $N - 2$. Consider the rows r and s corresponding to adjacent triangles $\Delta_r = (c, a, b)$ and $\Delta_s = (a, b, d)$:

$$V_{r,s} = \begin{bmatrix} w_b - w_a & w_c - w_b & w_a - w_c & 0 \\ 0 & w_d - w_a & w_b - w_d & w_a - w_b \end{bmatrix} \quad (9)$$

If the agents share the exact same expertise weight ($w_a = w_b$), the vectors become linearly dependent, dropping the rank of V below $N - 2$. The algebraic multiplicity of the zero eigenvalue increases, the system bifurcates, and global consensus is destroyed.

G Proof of Theorem 7

Assume H has a null space $\mathcal{N}(H)$ of dimension $m \geq 2$. Any state $x \in \mathcal{N}(H)$ satisfies $Hx = 0$. Consider the restriction of the system dynamics to this null space: $\dot{x} = \Omega x$.

Since Ω is real and skew-symmetric ($\Omega = -\Omega^\top$), its eigenvalues are purely imaginary. For any non-zero skew-form on an even-dimensional subspace, there exists an invariant 2D plane where the dynamics reduce to a standard harmonic oscillator: $\dot{x}_1 = \omega x_2$, $\dot{x}_2 = -\omega x_1$. The solutions to this subsystem are $x(t) = c_1 \cos(\omega t) + c_2 \sin(\omega t)$.

Because $Hx = 0$, there is no dissipation (no convergence) in these directions. The agents will oscillate endlessly along the boundary of the unresolvable subspace, producing circular critiques (hallucination loops) without ever reaching a stable fixed point.

H Proof of Theorem 8

By the corollary to Lemma 2, the vectors $\{\bar{v}_p\}_{p=1}^{N-2}$ together with $\mathbf{1}_N$ and w form a basis for the eigenspace of H . We obtain an orthonormal matrix $\theta = [u_1, u_2, \dots, u_N]$ via Gram-Schmidt Orthonormalization (GSO) on this basis. We choose $u_1 = \frac{\mathbf{1}_N}{\sqrt{N}}$. Thus, $\theta = \frac{1}{\sqrt{N}}[\mathbf{1}_N, w', \dots]$, where w' is the orthogonal projection of w ($w' = w - \frac{1}{N}\mathbf{1}_N$).

We define the perturbed symmetric matrix $\tilde{H} = H + \Delta$. By matrix perturbation theory, we analyze the (2, 2)-entry of $\theta^\top \Delta \theta$ to determine the shift of the

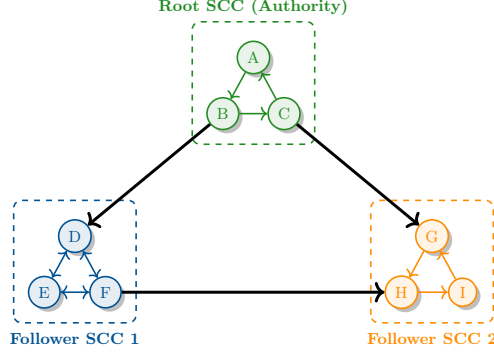


Fig. 10. Visualizing Theorem 9 (Condition 1: Authority). To achieve global consensus, the condensation of the directed graph must contain exactly one Root Strongly Connected Component (SCC). If multiple roots exist, the system bifurcates, and the algebraic multiplicity of the Laplacian’s zero eigenvalue exceeds 1.

secondary zero eigenvalue:

$$\begin{aligned}
 e_2^\top \theta^\top \Delta \theta e_2 &= \epsilon \left(\frac{w'^\top}{\sqrt{N}} \right) \tilde{w}_{ij} \mathbb{I}_{ij}^\top \left(\frac{w'}{\sqrt{N}} \right) \\
 &= \frac{\epsilon}{N} \left(w - \frac{1}{N} \mathbb{1}_N \right)^\top \tilde{w}_{ij} \mathbb{I}_{ij}^\top \left(w - \frac{1}{N} \mathbb{1}_N \right) \\
 &= \frac{\epsilon}{N^2} \left(\frac{1}{w_j} - \frac{1}{w_i} \right) (w_i - w_j) \\
 &= -\frac{\epsilon}{N^2} \frac{(w_i - w_j)^2}{w_i w_j}
 \end{aligned} \tag{10}$$

Since the targeted perturbation enforces an effective asymmetry ($w_i \neq w_j$), the term $-\frac{\epsilon}{N^2} \frac{(w_i - w_j)^2}{w_i w_j}$ is strictly negative (for positive initial weights). The rogue zero eigenvalue is strictly pushed into the stable left-half plane, collapsing the bifurcated eigenspace and guaranteeing a unique consensus manifold.

I Proof of Theorem 9

Necessity of C1: Two root SCCs will evolve independently, resulting in an algebraic multiplicity ≥ 2 for the zero eigenvalue of L_s . **Necessity of C2:** If unbalanced, by the Perron-Frobenius theorem applied to signed matrices, the spectral radius pushes eigenvalues of L_s into the left-half plane, causing divergence. **Sufficiency:** If C1 and C2 hold, $L_{unsigned}$ has a simple eigenvalue at 0 with right eigenvector $\mathbb{1}$. The right eigenvector of L_s is $v = D\mathbb{1}$. The system states converge to $cD\mathbb{1}$. If D contains both +1 and -1, this is a bipartite consensus (polarization). To achieve *unipolar* consensus, the final state must lie in

the span of $\mathbf{1}$. C3 ensures that the final projection $c = (w^\top x(0))/(w^\top D\mathbf{1})$ is uniquely well-defined, forcing the less expert faction to collapse into alignment with the more expert faction.

J Proof of Theorem 10

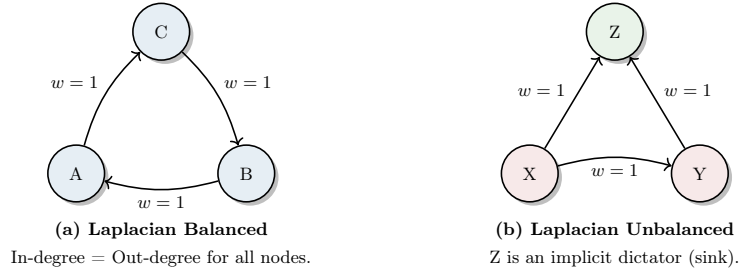


Fig. 11. Visualizing Laplacian Balance (Theorem 10). In (a), influence flows symmetrically, yielding true democratic consensus (the exact average of states). In (b), Agent Z only receives input and dominates the stationary distribution, pulling the consensus entirely to its initial state despite the uniform democratic setting $w = \mathbf{1}_N$.

Average consensus requires the left eigenvector associated with the zero eigenvalue of L_s to be $l^\top = \mathbf{1}_N^\top$. We evaluate $\mathbf{1}_N^\top L_s = \mathbf{1}_N^\top (\Delta - A) = 0$, which implies $\mathbf{1}_N^\top \Delta = \mathbf{1}_N^\top A$. Thus, the absolute in-degree must equal the absolute out-degree for all nodes.